

Velocity-Aligned Photofragment Dynamics: Stereodynamics in the Reaction $O(^1D) + N_2O \rightarrow NO + NO$

M. Brouard, S. P. Duxon, P. A. Enriquez, R. Sayos,[†] and J. P. Simons*

Chemistry Department, University of Nottingham, Nottingham NG7 2RD, UK (Received: February 7, 1991)

The secondary reaction of velocity aligned, superthermal atoms generated via molecular photodissociation can lead to aligned secondary reaction products. Their vector properties and their quantum state distributions can be measured by using Doppler resolved, polarized laser probe techniques. A simple LAB \rightarrow CM transformation can thus be used to determine the vector correlations among \mathbf{k} (the bimolecular collision velocity vectors), \mathbf{k}' (the reaction products' velocity vectors), and \mathbf{j}' (the reaction products' angular momenta). These are analogous to the (μ, ν, \mathbf{j}) correlations in the primary photodissociation. The strategy is demonstrated in a study of the dynamical stereochemistry of the reaction $O(^1D) + N_2O \rightarrow NO + NO$.

1. Introduction

Experimental strategies for probing the stereodynamics of molecular photodissociation have now attained a very high level of sophistication.¹ Among the most powerful (and productive) have been the development of Doppler-resolved, polarized, laser pump-probe methods for simultaneously acquiring scalar energy/quantum state distributions among the recoiling fragments; scalar and vector pair correlations between the energy and angular momentum disposals in the partner fragments; and vector correlations between the parent molecular transition dipole μ , the

fragments' recoil velocity ν , and angular momentum \mathbf{j} .²⁻⁵

Many simple molecular photodissociation systems generate velocity-aligned atomic fragments; if dissociation is prompt, the alignment is referenced to the LAB frame ($Z||\epsilon_p$) via the translational anisotropy, $\beta = 5\langle P_2(\hat{\nu} \cdot \hat{Z}) \rangle$. Prompt photodissociation implies a repulsive potential energy surface so that excitation near

(1) *Molecular Photodissociation Dynamics*; Adv. Gas Phase Photochem. Kinet.; Ashfold, M. N. R., Baggott, J. E., Eds.; Royal Society of Chemistry: London, 1972.

(2) Dixon, R. N. *J. Chem. Phys.* **1986**, *85*, 1866.

(3) Simons, J. P. *J. Phys. Chem.* **1987**, *91*, 5378.

(4) Houston, P. L. *J. Phys. Chem.* **1987**, *91*, 5388.

(5) Hall, G. E.; Houston, P. L. *Annu. Rev. Phys. Chem.* **1989**, *40*, 375.

[†] Present address: Departamento de Quimica Fisica, Universidad de Barcelona, 08028 Barcelona, Spain.

the Franck-Condon maximum generates superthermal fragments. When these are from a diatomic precursor, the atoms will be generated with a narrow velocity spread; the spread may be much broader, of course, when the partner species is a molecular fragment.

One of the best known examples is provided by the photodissociation of HBr at 193 nm, which (necessarily) generates very energetic H atoms travelling predominantly in directions aligned perpendicular to the polarization axis of the incident photon beam, i.e., with a translational anisotropy $\beta = -1$.^{6,7} Since their velocities are so large, their subsequent collisions with unreacted molecules in the bath gas, e.g., O₂ molecules at 300 K, closely approximate "superthermal beam-gas" collisions with near stationary target molecules. If the nascent bimolecular reaction products (e.g., OH(X)) are monitored under single-collision conditions via laser probing, the experiment effectively constitutes a *beam-gas study of bimolecular reaction dynamics in a bulb*. Doppler resolution of the polarized laser-induced fluorescence (or ionization) spectrum of the nascent products can allow determination of a second set of scalar distributions and vector correlations, initially referenced to the LAB frame ($Z||\epsilon_p$), but after a (simple) LAB \rightarrow CM transformation to the bimolecular collision frame, ($z||v$).

To what extent have these strategies been developed and realized? At the time of writing their application is only just beginning. Wolfrum reported strong rotational alignment of the OH molecules generated via the reaction of velocity aligned H atoms with O₂.⁸ A LAB \rightarrow CM transformation of his data, assuming a stationary target and the equivalence of \hat{k} (a unit vector along the collision velocity) and \hat{v} (a unit vector along the H atom recoil velocity), indicates an average rotational alignment $\langle P_2(\hat{J}'_{OH}\cdot\hat{k}) \rangle \simeq -1/2$, (vide infra).⁹ This corresponds to the limiting value expected for products rotating in the collision plane.³ Hancock and Orr-Ewing¹⁰ have derived formulas allowing for the loss of "reagent velocity definition" introduced by velocity spread in the atomic reagent and/or molecular target. Somewhat unexpectedly, they found no rotational alignment among the population of highly vibrationally excited CO molecules generated in the reaction of velocity aligned O(³P) atoms (generated by photodissociation of NO₂ at 355 nm, $\beta \sim -0.6$ ^{3,11}) with CS. Published reports of the alternative rotational alignment $\langle P_2(\hat{J}'\cdot\hat{k}) \rangle$ (equivalent to a (v, J) correlation in photodissociation fragments) have not yet appeared, though they should not be too long in coming. Bersohn and co-workers¹² have discovered a very strong translational alignment, specifically a $(k||k')$ correlation, of the *product* atoms generated in the "hot" atom displacement reaction



The possible operation of an inversion mechanism has been discussed.

The present work describes a preliminary stereodynamical study of the highly exothermic reaction

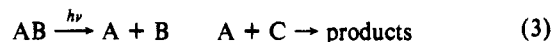


which follows the generation of superthermal, velocity aligned O(¹D) atoms via photodissociation of N₂O at 193 nm.¹³⁻¹⁵ Section

2 introduces the necessary formalism allowing transformation from the LAB \rightarrow CM frames and the determination of the product translational (k, k') and rotational (J', k) and (J', k') alignments from the laboratory data. Preliminary measurements of quantum state distributions and alignments in the NO molecules generated in reaction 2 are presented and discussed in section 4.

2. Theory

The photon-initiated reaction scheme may be represented by the equations



where $h\nu$ corresponds to a linearly polarized photon with polarization vector parallel to the laboratory Z axis ($\epsilon_p||Z$). Assuming, initially, that the species AB and C are stationary and that reactant A is generated via photodissociation with a single recoil velocity, then its velocity vector v may be equated with the relative velocity vector k of the collision. Following the notation of ref 16, let (θ, ϕ, χ) denote the Euler angles that describe the center-of-mass fixed axes (with $z||k$) relative to the space-fixed axes (with $Z||\epsilon_p$). For a given center-of-mass orientation (θ, ϕ, χ) the probability of collision can therefore be written

$$P(\theta, \phi, \chi) = [1 + \beta P_2(\cos \theta)]/8\pi^2 \quad (4)$$

where $\beta = 2\langle P_2(\hat{\mu}\cdot\hat{v}) \rangle \equiv 2\langle P_2(\hat{\mu}\cdot\hat{k}) \rangle$ and μ is the transition dipole moment of the AB molecule.

In the center-of-mass frame (with $z||k$) the angular distribution of the reaction products may be described by the spherical harmonic sum

$$f(\phi_m, \phi_m) = \sum_{kq} b_{kq} Y_{kq}(\theta_m, \phi_m) \quad (5)$$

where

$$b_{kq} = \int_0^{2\pi} \int_0^\pi Y_{kq}^*(\theta_m, \phi_m) f(\theta_m, \phi_m) \sin \theta_m d\theta_m d\phi_m$$

and again it is assumed that the reaction products are born with a single speed. The laboratory frame angular distribution of reaction products may be obtained by integrating the product of eqs 4 and 5 over all possible orientations of the center-of-mass frame.¹⁶ The resulting angular distribution may be written as a function of the polar and azimuthal angles θ_s, ϕ_s about Z:¹⁷

$$I(\theta_s, \phi_s) = C[1 + BP_2(\cos \theta_s)] \quad (6)$$

where

$$B = \beta \langle P_2(\cos \theta_m) \rangle = 5 \langle P_2(\cos \theta_s) \rangle$$

with $\cos \theta_m = \hat{k}\cdot\hat{k}'$ and $\cos \theta_s = \hat{\epsilon}_p\cdot\hat{k}'$. (Note that the absence of odd Legendre polynomials in eq 6 emphasizes that the photon-initiated reaction technique, using linearly polarized light, cannot be used to distinguish between forward and backward scattering in the molecule frame.)

If the photofragments (which are assumed for the moment to be rotationless) are probed via Doppler-resolved laser spectroscopy, then eq 6 may be rewritten in terms of the Doppler-broadened line-shape function $g(\bar{v})$:

$$g(\bar{v}) = C[1 + BP_2(\cos \theta_s)P_2(\chi_D)] \quad (7)$$

where θ_s is the angle between ϵ_p and k_s (the probe laser propagation direction) and χ_D , the relative displacement from line center, is defined as

$$\chi_D = \frac{c}{v} \frac{\bar{v}_0 - \bar{v}}{\bar{v}} = \frac{\bar{v}_0 - \bar{v}}{\Delta \bar{v}_D} \quad (8)$$

and has the limits $-1 \leq \chi_D \leq 1$.² In simulating experimental Doppler profiles, eq 7 must be convoluted with the probe laser line-shape function and with a Gaussian profile to accommodate

(16) Zare, R. N. *Angular Momentum: Understanding Spatial Aspects in Chemistry and Physics*; Wiley-Interscience: New York, 1988.

(17) Johnston, G. W.; Satyapal, S.; Bersohn, R.; Katz, B. *J. Chem. Phys.* **1990**, *92*, 206.

(6) Xu, Z.; Koplitz, B.; Wittig, C. *J. Phys. Chem.* **1988**, *92*, 5518.

(7) Magnotta, F.; Nesbitt, D.; Leone, S. R. *Chem. Phys. Lett.* **1981**, *83*, 21.

(8) Wolfrum, J. In *Selectivity in Chemical Reactions*; Whitehead, J. C., Ed.; Kluwer: Dordrecht, 1988; p 23.

(9) Brouard, M.; Simons, J. P., to be published.

(10) Green, F.; Hancock, G.; Orr-Ewing, A. J. *Faraday Discuss. Chem. Soc.*, in press.

(11) Busch, G. E.; Wilson, K. R. *J. Chem. Phys.* **1972**, *56*, 3626, 3638.

(12) Katz, B.; Park, J.; Satyapal, S.; Chattopadhyay, A.; Tasaki, S.; Yi, W.; Bersohn, R. *Faraday Discuss. Chem. Soc.*, in press.

(13) Chamberlain, G. A.; Simons, J. P. *J. Chem. Soc., Faraday Trans. 2* **1975**, *71*, 402.

(14) Goldstein, N.; Greenblatt, G. D.; Wiesenfeld, J. R. *Chem. Phys. Lett.* **1983**, *96*, 410.

(15) Honma, K.; Fujimura, Y.; Kajimoto, O.; Inoue, G. *J. Chem. Phys.* **1988**, *88*, 4739.

the smearing of the center-of-mass velocity vector, v_{CM} , induced by (isotropic) thermal motions in the AB precursor and C target molecules. The full width at half-maximum of this Gaussian will be

$$fwhm = \left[\left(\frac{M_A}{M_{AC}} \Delta v_{AB} \right)^2 + \left(\frac{M_C}{M_{AC}} \Delta v_C \right)^2 \right]^{1/2} \quad (9)$$

where Δv_{AB} and Δv_C are the Doppler widths of the AB and C molecules. It is noted in passing that both the magnitude¹⁸ and the angular distribution¹⁰ of the relative velocity vector, \mathbf{k} , will also be smeared by thermal motions of AB and C (and by any distribution of speeds in reactant A generated in the photodissociation process). These effects are not included in the convolution represented by eq 9 but are considered in more detail in refs 10 and 18.

Derivation of the classical angular distribution of reaction product rotational vectors, \mathbf{j}' , follows a procedure analogous to that outlined above, yielding

$$I(\theta_s', \phi_s') = C' [1 + AP_2(\cos \theta_s')] \quad (10)$$

where

$$A = \beta \langle P_2(\cos \theta_m') \rangle = 5 \langle P_2(\cos \theta_s') \rangle$$

with $(\cos \theta_m') = \hat{\mathbf{k}} \cdot \hat{\mathbf{j}}'$ and $(\cos \theta_s') = \hat{\mathbf{e}}_p \cdot \hat{\mathbf{j}}'$. (Note that in both eqs 6 and 10, the factor $\beta/5$ may be equated with $\langle P_2(\hat{\mathbf{e}}_p \cdot \hat{\mathbf{k}}) \rangle$ and arises from the laboratory to molecule frame transformation.) In terms of the rotational alignment parameter, $A_0^{(2)}$, defined as^{2,16}

$$A_0^{(2)} = 2 \langle P_2(\hat{\mathbf{e}}_p \cdot \hat{\mathbf{j}}') \rangle$$

it follows that

$$A_0^{(2)} = \frac{2}{5} \beta \langle P_2(\hat{\mathbf{k}} \cdot \hat{\mathbf{j}}') \rangle = \frac{2}{5} A \quad (11)$$

in the high- \mathbf{j} limit. As mentioned above, the effects of a distribution of reagent relative velocity vectors, \mathbf{k} , on the form of eqs 10 and 11 has been considered by Hancock and co-workers.¹⁰

The analysis outlined above does not include all the vector correlation properties that can be obtained via Doppler-resolved probing of photon-initiated bimolecular collision/reaction products. As with direct photodissociation studies,² a total of nine bipolar moments are required to characterize fully the correlated angular distributions of \mathbf{j}' and \mathbf{k}' about \mathbf{e}_p when linearly polarized photolysis and probe radiation is employed. The method of extracting these moments from the Doppler broadened profiles will be identical with the procedure employed in photodissociation studies:¹⁹ eqs 6 and 10 merely provide a means of interpreting the translational anisotropy and rotational alignment data. Two further correlations, expected to make a significant contribution to the Doppler line shapes observed in reactive studies, are characterized by the moments $\beta_{\mathbf{k}\mathbf{j}}^{\nu}$ and $\beta_{\mathbf{k}\mathbf{j}}^{\mu}$ [these are analogous to $\beta_0^{\nu}(22)$ (the (\mathbf{v}, \mathbf{j}) correlation) and to $\beta_0^{\mu}(22)$ (the $(\mu, \mathbf{v}, \mathbf{j})$ correlation) in the primary fragments derived from photodissociation]. While sensitivity to $\beta_{\mathbf{k}\mathbf{j}}^{\nu}$ will depend on the magnitude of the translational anisotropy (β) of the reactant A, this is not the case for $\beta_{\mathbf{k}\mathbf{j}}^{\mu}$: its determination in a reactive system will thus provide a direct insight into the nature of the nuclear motions in the bimolecular transition-state region.

3. Experimental Section

The laser system comprised a polarized excimer photolysis laser ($\lambda \sim 193$ nm, ≤ 40 mJ pulse⁻¹) and an electronically delayed excimer pumped dye laser ($\lambda \sim 225$ –500 nm) that had an etalon-narrowed bandwidth at the fundamental of ~ 0.04 cm⁻¹. The NO reaction products were probed via the ($A^2\Sigma \leftarrow X^2\Pi$) and ($B^2\Pi \leftarrow X^2\Pi$) transitions on the $0 \leftarrow v'' \leq 10$ and $(0-2 \leftarrow v'' \leq 20)$ vibronic bands, respectively. Laser-induced fluorescence from NO($A^2\Sigma$) was observed through an interference filter centered on the 0-0 band, while emission from the $B^2\Pi$ state was

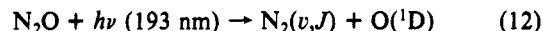
viewed through a broadband (225–500 nm) filter. Photomultiplier signals were averaged on a boxcar and transferred to a micro-computer for normalization to the probe laser power and signal averaging. As in previous photodissociation studies,¹⁹ rotational alignments were obtained from the integrated relative intensities of $Q \uparrow$ and $P, R \uparrow$ transitions in the two pump-probe coaxial geometries with $\epsilon_p \parallel \epsilon_a$ (case A) and $\epsilon_p \perp \epsilon_a$ (case B) with the fluorescence detected along ϵ_a . Doppler-resolved profiles were also recorded in geometries A and B as well as in geometry case D for which $\epsilon_p \parallel \mathbf{k}_a$ and $\mathbf{k}_p \perp \mathbf{k}_a$.

Unless otherwise stated, typical delay times between the photolysis and probe pulses were ≤ 200 ns. At these delay times and with pressures of (slowly flowing) N₂O in the range 50–200 mTorr, sufficient NO signals could be obtained while ensuring the absence of any observable relaxation of the products. No NO signals could be detected at delay times less than 50 ns at pressures ~ 30 mTorr, and their rates of growth at longer delays were consistent with the known room-temperature rate constant for the reaction of O(¹D) with N₂O.²⁰ These observations demonstrate that all the NO generated, regardless of the vibrational level populated, arose from photon-initiated reaction rather than from direct photodissociation of N₂O and that there was no residue of relaxed NO remaining in the probed region from previous laser shots.

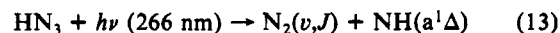
4. Results and Discussion

The highly exothermic reaction of O(¹D) with N₂O, which proceeds with near-unit collision efficiency,²⁰ can generate NO molecules in very highly excited rovibrational levels.^{13,14} Fully dispersed LIF spectra of the NO generated under single-collision conditions have now been recorded for all vibrational levels in the range $v = 0$ –18, though their complete spectral assignment proves to be a challenge. Those produced in the lower lying levels and detected via the A–X γ -band system can be fully assigned, but in the very highly excited vibrational levels, detected predominantly via the B–X β -band system, where spectral congestion is most severe, full assignment is a herculean task; to date vibrational assignments only have been possible and then only by allowing sufficient time for partial (rotational) relaxation to promote the required spectral decongestion. Representative LIF spectra for this region are shown in Figure 1.

The exothermicity of the bimolecular reaction (2) is sufficient only to excite the NO product molecules into vibrational levels $v \leq 16$. Population of rotationally excited levels in $v = 18$ requires an additional collision energy $\langle E_{CM} \rangle \approx 70$ kJ mol⁻¹. Clearly, the reaction must proceed at elevated mean collision energies, which can be carried only by the reagent O(¹D) atoms generated in the initial photodissociation step:



If the N₂ molecules were generated with no internal excitation, the total kinetic energy release would be 340 kJ mol⁻¹ and the mean center-of-mass collision energy of O(¹D) with N₂O would be $\langle E_{CM} \rangle \approx 159$ kJ mol⁻¹, sufficient to generate NO molecules excited into vibrational levels $v \leq 24$. If, however, generation of the molecules excited into $v \leq 18$ is taken to represent the limit imposed by energy conservation, the total kinetic energy released in (3) cannot exceed 152 kJ mol⁻¹. This is consistent with the primary production of N₂ ($v = 0, J < 90$) and $\langle f_R \rangle_{N_2} < 0.55$. The electronic state(s) accessed by absorption at 193 nm are thought to be nonlinear²¹ so very high rotational excitation of the N₂ is predictable; indeed in the photodissociation of the analogous, isoelectronic molecule, HN₃



the N₂ is generated primarily in $v = 0$, with $\langle J \rangle \approx 70$ and $\langle f_R \rangle_{N_2} \approx 0.48$.^{22,23} While measurement of the limiting energy disposal

(20) Donovan, R. J.; Husain, D. *Chem. Rev.* 1970, 70, 489.

(18) Van der Zande, W. J.; Zhang, R.; Zare, R. N.; McKendrick, K. G.; Valentini, J. J. *J. Phys. Chem.*, this issue.

(19) August, J.; Brouard, M.; Simons, J. P. *J. Chem. Soc., Faraday Trans. 2* 1988, 89, 587.

(21) Ashfold, M. N. R.; Macpherson, M. T.; Simons, J. P. In *Topics in Current Chemistry*; Boschke, F. L., Ed.; Springer-Verlag: Berlin, 1979; Col. 86, p 1.

(22) Gericke, K.-H.; Theinl, R.; Comes, F. J. *J. Chem. Phys.* 1990, 92, 6548.

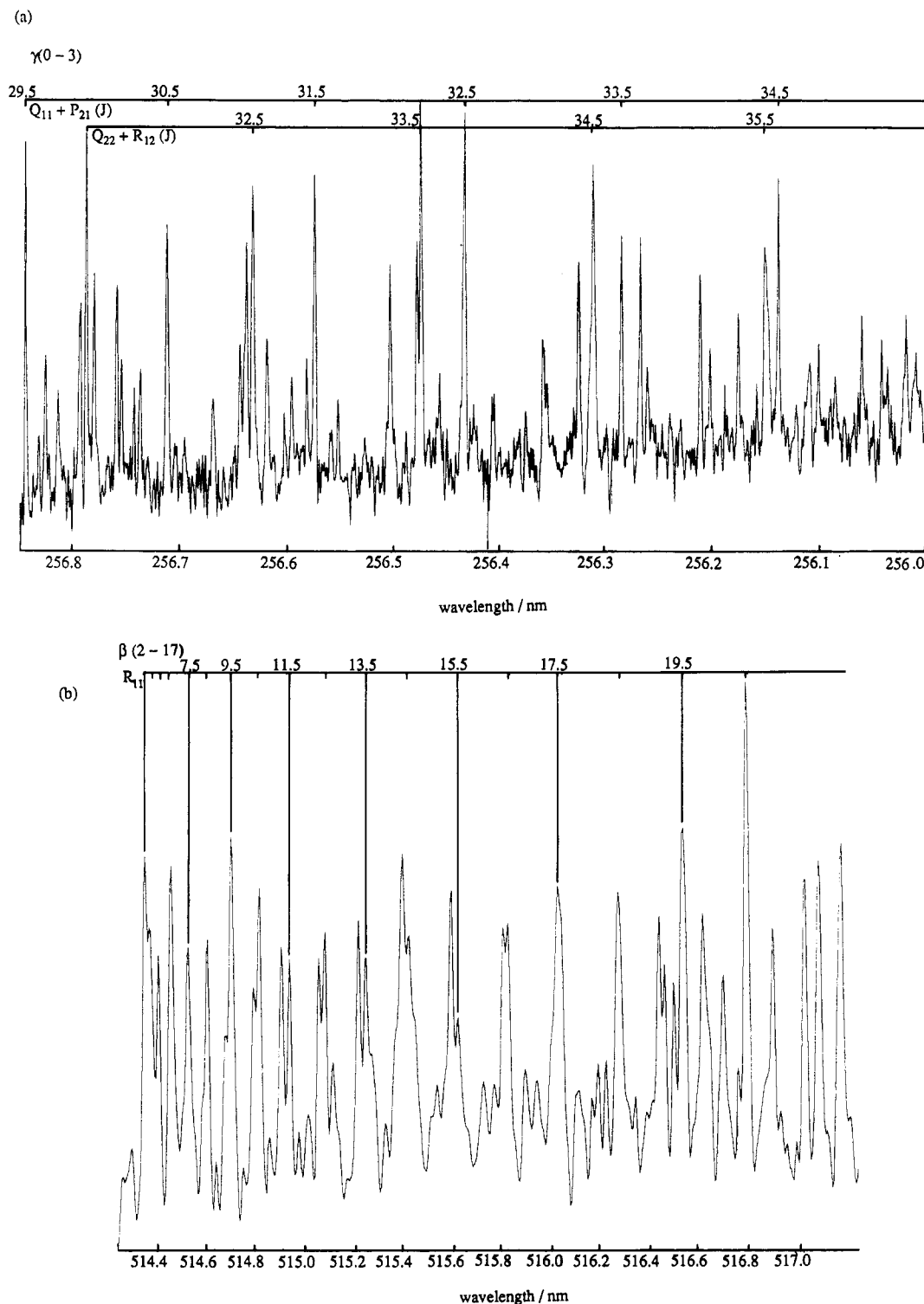


Figure 1. LIF spectra of vibrationally excited NO, generated via reaction of superthermal O(¹D) atoms with N₂O: spectra recorded under (a) single collision and (b) partially relaxed conditions.

in the secondary bimolecular reaction (2) cannot replace a direct measurement of the energy disposal in the primary photofragments, it does provide a qualitative guide and also establishes an estimate of the mean center-of-mass collision energy. Future experiments, employing REMPI detection of the internal quantum state distribution in the N₂,²³ will hopefully yield a quantitative estimate.

A full analysis of the quantum state distributions among the several thousand populated rovibrational levels populated in the bimolecular reaction products is a daunting prospect, and to keep matters simple, the first detailed measurements have been focused

on the NO molecules produced in $v = 0$, particularly, and the contrast with those found in vibrational levels $v = 1, 3$, and 10 . The contrast could not be more dramatic. NO molecules produced in $v = 0$ are *both* rotationally unexcited, with a mean rotational temperature $T_R \approx 320$ K (see Figure 2) *and* translationally cold, with a narrow Doppler width $\Delta\nu_D \approx 0.044$ cm⁻¹ (see Figure 3a) corresponding to a LAB velocity of ~ 300 ms⁻¹ and a LAB kinetic energy ~ 110 cm⁻¹. In contrast all NO molecules produced in vibrational levels $v > 0$ are rotationally highly excited; those in $v = 1$, for example, have a mean rotational temperature $T_R \approx 5500$ K (see Figure 2), and those in higher vibrational levels appear to carry even higher rotational excitation. They also carry rather higher translational energies since the Doppler widths of individual

(23) Chu, J. J.; Marcus, P.; Dagdigan, P. *J. Chem. Phys.* **1990**, *93*, 257.

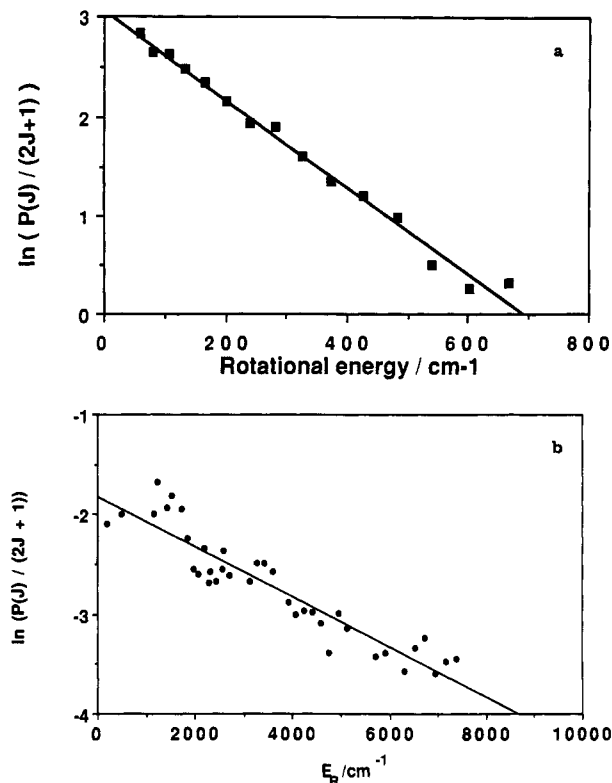


Figure 2. Rotational population distributions in $\text{NO}(X^2\pi_{1/2})$ generated in the reaction of superthermal $\text{O}(^1\text{D})$ atoms with N_2O : (a) $v = 0$, (b) $v = 1$.

TABLE I: Approximate Energy Disposals in Selected Vibrational States of NO Generated via the Reaction

$\text{O}(^1\text{D}) + \text{N}_2\text{O} \rightarrow \text{NO}(v_1) + \text{NO}(v_2)$				
v_1	E_{v_1}, cm^{-1}	$\langle E_R \rangle, \text{cm}^{-1}$	$\langle E_T \rangle^{\text{LAB}}, \text{cm}^{-1}$	$\langle v_2 \rangle$
0	0	200	110	16–18
1	1876	4000	690	≤ 17
3	5540	>4000	1350	≤ 13
10	17600	not determined	1280	≤ 4

rotational lines are all greater than for $\text{NO}(v = 0)$ (see Figure 3). Energy disposal data for the levels $v = 0, 1, 3$, and 10 are summarized in Table I.

Energy conservation requires the NO molecules generated in $v = 0$ to be partnered only by NO molecules carrying very high levels of rovibrational excitation. Furthermore, the narrowness of the Doppler profile shown in Figure 3a reflects a narrow spread of internal energies in the partner molecules, and it is likely that these correspond principally, to the NO molecules produced in the “super-excited” levels $16 < v \leq 18$. The spread of population among these levels must reflect the spread of collision energies in the hot $\text{O}(^1\text{D})$ reaction, rather than a spread of population associated with a specific collision energy. The simplest dynamical interpretation of these data is the assumption of a “near-stripping” mechanism for the reaction channels generating $\text{NO}(v=0)$, with the unexcited NO behaving as the spectator associated with the “old” N–O bond in the target molecule. New experiments with isotopically labeled $^{15}\text{N}^{14}\text{NO}$ (refs 13, 15) should provide confirmatory evidence.

The channels generating NO in vibrational levels $v = 1-3$ must also generate sister molecules with high rovibrational excitation, but the large jump in their rotational and translational energies, cf. $\text{NO}(v=0)$, suggests an increasing contribution from an alternative microscopic mechanism. The energy balance for the channels producing $\text{NO}(v=10)$ (based on the Doppler profile for the rotational level $N = 26$) shown in Figure 3d, yields $\text{NO}(v \leq 4)$ as the most likely sister product.

Vector Correlations. Figure 4 shows the LAB rotational alignments of the NO molecules generated in $v = 0$, for $J = 5.5$

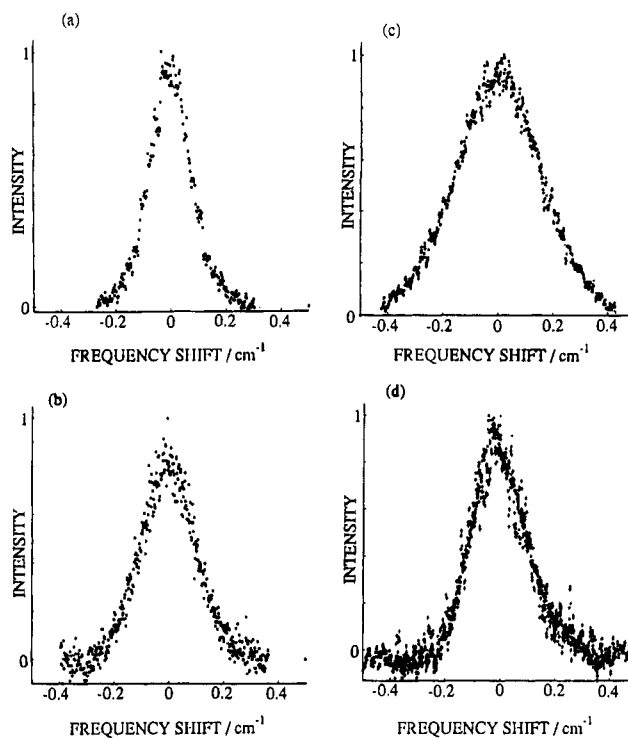


Figure 3. Doppler profiles of selected rotational features in the LIF spectrum of $\text{NO}(X^2\pi_{1/2})$: (a) $v = 0, N = 20$; (b) $v = 1, N = 35$; (c) $v = 3, N = 31$; all case A. (d) $v = 10, N = 26$; case A, circles; case D, crosses.

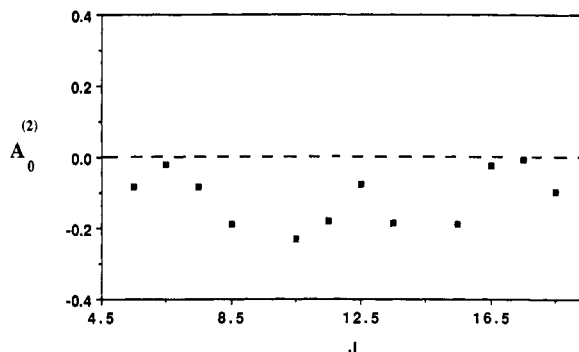


Figure 4. Rotational alignments in $\text{NO}(X^2\pi_{1/2}), v = 0$, generated in the reaction of velocity aligned $\text{O}(^1\text{D})$ with N_2O .

to 18.5; despite the scatter they are all negative and the mean alignment for levels with $J \geq 10.5$ is $A_0^{(2)} \approx -0.1$. Assuming the cold NO in $v = 0$ to be the spectator product of a stripping collision, no rotational alignment would have been anticipated. There must be some residual interaction between the two nascent NO fragments in the reaction transition state. The most plausible origin of the alignment is via angular momentum transfer from orbital motion associated with the velocity-aligned reagent $\text{O}(^1\text{D})$ atoms, into rotation of the collision complex. Note that the measurement of a nonzero rotational alignment also establishes a translational alignment in the reagent atoms: if their mean translational anisotropy $\bar{\beta}$ were zero, all LAB alignments of the NO product molecules would necessarily be zero (cf. eqs 6 and 11). Assuming rotational alignment of the “old” NO product molecules to result from angular momentum transfer leads to the expectation $\langle P_2(\hat{\mathbf{k}} \cdot \hat{\mathbf{j}}) \rangle < 0$. With $0 \geq \langle P_2(\hat{\mathbf{k}} \cdot \hat{\mathbf{j}}) \rangle \geq -1/2$ the mean translational anisotropy, $\bar{\beta}$, of the $\text{O}(^1\text{D})$ atoms must be positive, lying within the bounds $2 \geq \bar{\beta} \geq 1/2$. When it has been possible to assign the rotational transitions associated with the “new” NO molecules, $\text{NO}(v \sim 20)$, and to measure their rotational alignments (which could approach the limiting values $A_0^{(2)} \geq -2/5$ for $\bar{\beta} \leq +2$), it will be possible to define the limits to $\bar{\beta}$ rather more precisely. The separate determination of $\bar{\beta}$ via Doppler-resolved REMPI spectral probing of the N_2 molecules accompanying the velocity

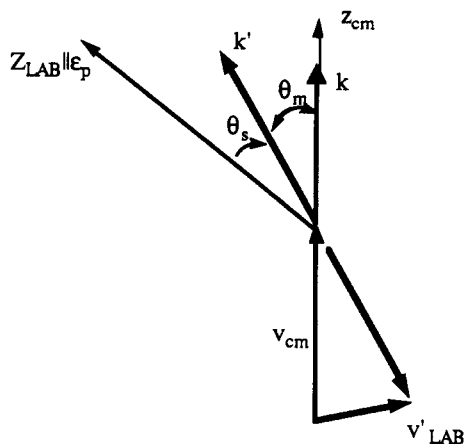


Figure 5. Schematic Newton diagram for the collision of superthermal velocity aligned atoms, with a stationary target molecule.

aligned O(¹D) will complete the picture, to give the true CM alignments in the scattered NO products.

The operation of a "near" stripping mechanism would imply a CM scattering angle $\theta_m \sim 0$ and a LAB translational alignment $B^{NO} \simeq \beta$ (cf. eq 6). An appropriate schematic Newton diagram is shown in Figure 5. In principle, it should be possible to estimate this alignment from the dependence of the Doppler-resolved spectral line shapes on the excitation-detection geometry, e.g., $k_p \parallel k_s$ vs $k_p \perp k_s$. Unfortunately the NO($\nu=0$) is so slow moving that its associated Doppler width is comparable with the available experimental resolution (see Figure 3a). This should not be a problem with the highly rovibrationally excited sister products. Forward scattering from a "near" stripping collision should endow them with LAB velocities $\lesssim 2v_{CM} \simeq 1.8 \text{ km s}^{-1}$ (see Figure 5).

The experimental resolution has not been restrictive in probing the NO populations in the intermediate vibrational levels, for example, those generated in $\nu = 10$ —the principle partners of those generated in $\nu = 3$. Doppler profiles recorded for NO($\nu=10$) under coaxial (case A) and perpendicular (case D) excitation-detection geometries can be compared in Figure 3d. They are identical, within the experimental precision, implying a near isotropic angular distribution in this channel, since $\beta \neq 0$.

A simplistic mechanism that could result in the rovibrational excitation of *both* partners and accounts for their isotropic angular distribution and for the relatively low kinetic energy release is reaction via a short-lived complex. This behavior could not be accommodated by an impulsive "ballistic" mechanism associated with the superthermal atomic collisions.

Figure 6 shows the Λ -doublet population ratios, $\pi(A'')/\pi(A')$ in NO($\nu=0$) determined for the rotational levels $J = 10.5$ – 18.5 . They are all less than unity and decrease with increasing J . Extrapolating the data to the high- J limit²⁴ yields a population ratio $\pi(A')/\pi(A'') = 2 \pm 0.7$, i.e., a preference for the half-filled π -electron orbital lobe to lie in the plane of rotation. If the weak rotational alignment of NO($\nu=0$) arises from collisional angular momentum transfer, then the small preference for electronic orbital alignment suggests a tendency for the half-filled-lobe to lie in the plane of the collision. Interesting (as yet, unanswered) questions

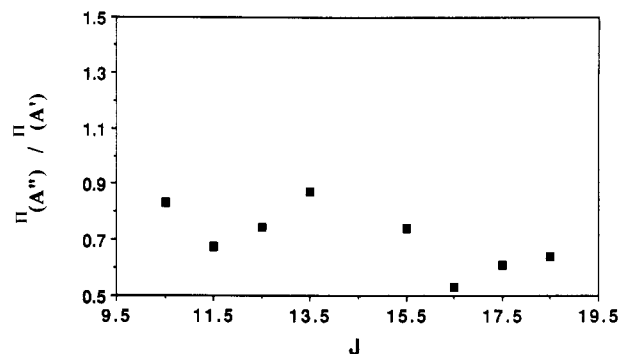


Figure 6. Relative Λ -doublet populations in NO($X^2\pi_{1/2}$), $\nu = 0$, generated via reaction of O(¹D) with N₂O.

are the degree of electronic orbital alignment that might be introduced by the velocity aligned reagent O(¹D) atoms and the degree to which it might influence the orbital alignment in the products. Examples of orbital selectivity *either* in reagent atoms *or* in product molecules are widely available,²⁵ but a full state-to-state study would be especially valuable since it could trace the preferred movement of electron density in the course of a reactive collision.

5. Conclusion

These preliminary experiments have shown how velocity-aligned "hot" atoms, generated via polarized laser photodissociation, can be used to probe the state-selected, stereodynamics of their subsequent bimolecular reactions. Their success encourages the development of a new experimental strategy in which the power of high-resolution, polarized laser pump-probe techniques can supplement the traditional crossed molecular beam experiment to reveal the detailed anatomy of reactive (and inelastic) atomic and molecular collisions.

Dedication

One of us (J.P.S.) first met Dick Bernstein after a brilliant Hinshelwood Lecture in Oxford.²⁶ His excitement and enthusiasm were utterly infectious. Many meetings followed: in Jerusalem at a seminal Workshop on Dynamical Stereochemistry,²⁷ in the English Lake District at a NATO Advanced Research Workshop,²⁸ and at home in Los Angeles. They were not enough. This little paper is a small reflection of the inspiration he generated during those brief encounters.

Acknowledgment. R.S. thanks the British Council and the Spanish Ministry of Education and Science for the award of a Fleming Fellowship; P.A.E. thanks the Spanish Ministry of Education and Science for postgraduate research support.

Registry No. N₂O, 10024-97-2; O, 17778-80-2; NO, 10102-43-9.

(25) *Orientation and Polarisation Effects in Reaction Collisions*; Faraday Symposium 24; *J. Chem. Soc., Faraday Trans. 2* **1989**, *85*, 925–1376.

(26) Bernstein, R. B. *Chemical Dynamics via Molecular Beam and Laser Techniques*; The Hinshelwood Lectures, Oxford, 1980; Clarendon Press: Oxford, 1982.

(27) *Dynamical Stereochemistry Issue J. Phys. Chem.* **1987**, *91*, 5365–5516.

(28) *Selectivity in Chemical Reactions*; Whitehead, J. C., Ed.; Kluwer: Dordrecht; 1988; 1.

(24) Andresen, P.; Rothe, E. W. *J. Chem. Phys.* **1985**, *82*, 3634.